between 340 and 380 nm.[9] Nitrous acid, produced from the N(III) product of the first-order reaction and trace water, appears to be the chain propagator, as was noted[4] in decomposition in acidic, aqueous solutions, where the overall stoichiometry was represented as

$$4\mathrm{ON(SO_3)_2}^{2-} + 3\mathrm{H_2O} \rightarrow 2\mathrm{HON(SO_3)_2}^{2-} + \mathrm{N_2O} + 4\mathrm{SO_4}^{2-} + 4\mathrm{H}^+$$

In this study, at the low concentrations of nitrosyldisulfonate used, no gas bubbles were observed so this stoichiometry was not confirmed for the rapid decomposition products.

Conclusions

Care must be used in selecting and purifying the solvents to be used in studies involving the nitrosyldisulfonate free-radical anion. The only nonaqueous solvent found for potassium nitrosyldisulfonate (the most readily prepared salt) was DMSO; however, it could never be dried well enough to prevent the chain decomposition process. If an inhibitor of potassium sulfamate and sulfamic acid were added to consume nitrous acid, the chain process was stopped, which otherwise would lead to complete decomposition in about $2^1/_2$ h, and the reaction proceeded by a slow first-order process with a rate constant of about 10^{-5} s^{-1} at 25 °C.

The other solvents used required the tetraphenylarsonium salt and exhibited the rather rapid chain reaction also, unless dried very carefully. This salt decomposed more slowly than did the tetraphenylstibonium salt under the same conditions.

Water seemed to have little effect on the slow first-order decomposition, but its presence promoted the chain process which rapidly leads to complete loss of the radical.

For those uses of nitrosyldisulfonate ion radical that involve a period of time the reaction products must be considered also. The products of the slow first-order decomposition were found to be nitrite, hydroxylaminedisulfonate, and hydroxylaminetrisulfonate ions. The much more rapid chain process was found to produce hydroxylaminedisulfonate and sulfate ions. Other products remain unidentified.

The products of the first-order process are about the same as those obtained by decomposition in mildly alkaline aqueous solutions and probably are formed by the mechanism

$$\mathrm{O\dot{N}(SO_3)_2}^{2-} \xrightarrow{k_1} \mathrm{O\dot{N}SO_3} + \mathrm{SO_3}^{2-} \tag{1}$$

$$\mathrm{O\dot{N}SO_3} \xrightarrow{k_2} \mathrm{NO}^+ + \cdot\mathrm{SO_3}^- \tag{2}$$

$$\mathrm{O\dot{N}(SO_3)_2}^{2-} + \mathrm{SO_3}^{2-} \xrightarrow{k_3} {}^-\mathrm{ON(SO_3)_2}^{2-} + \cdot\mathrm{SO_3}^- \tag{3}$$

$$2[\mathrm{O\dot{N}(SO_3)_2}^{2-} + \cdot\mathrm{SO_3}^- \xrightarrow{k_4} \mathrm{ON(SO_3)_3}^{3-}] \tag{4}$$

$$4\mathrm{O\dot{N}(SO_3)_2}^{2-} \rightarrow \mathrm{NO}^+ + {}^-\mathrm{ON(SO_3)_2}^{2-} + 2\mathrm{ON(SO_3)_3}^{3-}$$

The initial breaking of an N–S bond is proposed as the rate-determining step of the overall reaction. Reaction 2 is fast relative to reaction 1 as no detectable amounts of any other radicals were observed. Reactions 3 and 4 are known[10] to be much faster than the observed rate of color loss in this study. Applying steady-state assumptions and assuming that k_2, k_3, and k_4 are large in comparison to k_1 the observed first-order rate constant for color loss is equal to $4k_1$.

The NO^+ formed could react with traces of water to form nitrous acid which was found to be the chain propagation for rapid decomposition in acidic solutions; hence use of an inhibitor or very dry solvent prevents this fast reaction and permits the radical to decompose by the slow first-order process.

Registry No. $\mathrm{ON(SO_3)_2}^{2-}$, 15177-44-3; $\mathrm{ON(SO_3)_2}^{2-}$-$((\mathrm{C_6H_5})_4\mathrm{Sb}^+)_2$, 20475-16-5; $\mathrm{ON(SO_3)_2}^{2-}$-$((\mathrm{C_6H_5})_4\mathrm{As}^+)_2$, 20582-58-5.

References and Notes

(1) (a) Presented in part at the 161st National Meeting of the American Chemical Society, Los Angeles, Calif., April 1971; see Abstracts, No. INOR 144. (b) Brigham Young University. (c) NSF Trainee, 1968–1971; Ph.D. Thesis, Brigham Young University, 1971. (d) Preliminary work on this study done as a M.A. candidate at Vanderbilt University, 1965; M.A. Thesis, 1965.
(2) W. Moser and R. A. Howie, *J. Chem. Soc. A*, 3039 (1968).
(3) D. L. Fillmore and B. J. Wilson, *Inorg. Chem.*, **7**, 1592 (1968).
(4) J. H. Murib and D. M. Ritter, *J. Am. Chem. Soc.*, **74**, 3394 (1952).
(5) B. J. Wilson and D. M. Ritter, *Inorg. Chem.*, **2**, 974 (1963).
(6) J. Chatt and F. G. Mann, *J. Chem. Soc.*, 1192 (1940).
(7) J. Bjerrum and J. P. McReynolds, *Inorg. Synth.*, **2**, 216–217 (1946).
(8) W. C. Bray, M. E. Simpson, and A. A. MacKenzie, *J. Am. Chem. Soc.*, **41**, 1363 (1919).
(9) T. A. Turner and G. A. Wright, *Chem. Rev.*, **59**, 497 (1959).
(10) J. C. M. Li and D. M. Ritter, *J. Am. Chem. Soc.*, **75**, 5831 (1953).

Contribution from the Department of Chemistry,
University of Western Ontario, London, Ontario N6A 5B7, Canada

Molecular Structure and Absolute Configuration of (−)$_{280}$-*cis*-Dichloro(1-methylamino-2(*S*)-aminopropane)platinum(II)

RICHARD G. BALL, NANCY J. BOWMAN, and NICHOLAS C. PAYNE*

Received September 15, 1975 AIC50684D

The molecular structure and absolute configuration of (−)$_{280}$-*cis*-dichloro(1-methylamino)-2(*S*)-aminopropane)platinum(II), $\mathrm{Cl_2Pt(CH_3NHCH_2CHCH_3NH_2)}$, have been determined from three-dimensional x-ray data collected by counter methods. The molecule crystallizes in the orthorhombic space group $P2_12_12_1$ with four formula units per cell. The unit cell dimensions are a = 10.488 (3), b = 11.034 (4), and c = 7.432 (2) Å. The structure has been refined by full-matrix least-squares techniques on F, using 3297 unique reflections for which $F^2 > 3\sigma(F^2)$, to a final agreement factor of 0.035. The complex is square planar with an average Pt–Cl distance of 2.303 (3) Å and an average Pt–N distance of 2.021 (8) Å. The absolute configuration of the chelate ring as determined by the Bijvoet absorption-edge technique is δ, and the N-methyl substituent is in the axial position.

Introduction

The conformation adopted by the five-membered chelate ring formed upon coordination of a substituted ethylenediamine ligand to a metal atom is generally dictated by the nonbonding interactions associated with the puckered ring.[1] Thus most C-substituted ethylenediamine ligands in octahedral complexes adopt a gauche conformation, with the substituent in the equatorial position. In the case of N-substituted ethylenediamine ligands in monodiamine and *trans*-bis(diamine) complexes of Co(III), the substituent was also shown by ^{1}H NMR and circular dichroism studies[2] to adopt preferentially the equatorial position. More recently, a conformational analysis[3] suggested that the free energy difference between the axial and the equatorial substituents was small in octahedral monodiamine complexes, and ^{1}H NMR and circular dichroism studies of platinum(II) complexes of methylglycines[4] indicated that at equilibrium there was a significant amount of the axial isomer present. Equilibrium constants for the axial–equatorial distribution of the *N*-methyl group in a number of 1-methylamino-2(*S*)-aminopropane complexes of Pt(II) and Pt(IV) have been determined by Bosnich and Sullivan,[5] who showed that there is little difference in free energies between the two diastereoisomers. Thus reaction of 1-methylamino-2(*S*)-aminopropane with K_2PtCl_4 gave two yellow crystalline modifications (needles and equidimensional "blocks") of a compound of composition $Cl_2Pt(CH_3NHCH_2CHCH_3NH_2)$. The two forms have nearly identical linear absorption spectra, but almost enantiomorphic circular dichroism spectra. They have similar low solubilities in water but are easily separated mechanically. As part of our interest[6] in determining the molecular structures and absolute configurations of optically active transition metal complexes and relating the spatial orientations of the various sources of dissymmetry to the observed circular dichroism spectra, we have undertaken the single-crystal x-ray analysis of the two crystalline modifications of *cis*-$[Cl_2Pt(CH_3NHCH_2CHCH_3NH_2)]$. We report here the molecular structure and absolute configuration of the equidimensional "blocks" modification, which is shown to contain the *N*-methyl substituent occupying the axial position.

Experimental Section

Samples of both crystalline modifications of dichloro(1-methylamino-2(*S*)-aminopropane)platinum(II) were kindly supplied by Bosnich and Sullivan.[5] Crystals suitable for diffraction analysis of the pale yellow equidimensional "blocks" modification were selected, and preliminary Weissenberg and precession photography showed them to be orthorhombic with Laue symmetry *mmm*. The systematic extinctions observed, *h*00 for *h* odd, 0*k*0 for *k* odd, and 00*l* for *l* odd, are consistent only with space group $P2_12_12_1$, $D_2{}^4$, No. 19.[7]

The crystal chosen for data collection had approximate dimensions 0.24 mm × 0.21 mm × 0.18 mm. It was carefully measured on a microscope fitted with a filar eyepiece in anticipation of an absorption correction. The crystal possessed 12 faces of the forms {110}, {101}, and {011} as determined by optical goniometry, the most prominent being (110) and ($\bar{1}\bar{1}0$). The crystal was mounted in a general orientation, with [$\bar{1}$10] offset some 10° from the diffractometer ϕ axis.

A least-squares refinement[8] of 24 intense, carefully centered reflections with 2θ ranging between 18 and 38°, using Mo radiation ($\lambda(K\alpha_1)$ 0.709 26 Å), at 19 °C gave cell dimensions of a = 10.488 (3), b = 11.034 (4) and c = 7.432 (2) Å. The density, measured by flotation in a mixture of ethylene bromide and diiodomethane, is 2.706 (1) g cm^{-3}. This agrees reasonably well with the value of 2.734 g cm^{-3} calculated assuming $Z = 4$. Several ω scans of strong, low-angle reflections were recorded to examine the crystal mosaicity. The average width at half-height was 0.07°, which was judged acceptable.[9]

Intensity data were collected on a computer-controlled Picker FACS-1 diffractometer. The θ–2θ scan technique employing Mo $K\alpha$ radiation prefiltered with 0.07-mm Nb foil was used. The tube takeoff angle was 2.0°. A scan rate of 1°/min was employed. A symmetric scan width of 0.8° was used for reflections with $2\theta < 45°$ and a width of 1.0° for those above 45°. The scan width was automatically corrected for α_1–α_2 dispersion. Stationary-crystal, stationary-counter background counts were taken at each end of the scan for 10 s for reflections with $2\theta < 65°$ and 20 s for all higher angle reflections. The aperture, with an opening of 0.4 × 0.4 cm, was positioned directly in front of the counter and 30 cm from the crystal.

Intensities of 4920 reflections were recorded in the range $2.5 < 2\theta < 75°$ for reflections *hkl* and *hk$\bar{l}$*. Six reflections, 02$\bar{1}$, 040, 021, 0$\bar{4}$0, 020, and 004, were chosen as standards and their intensities were measured every 200 reflections as a check on machine and crystal stability. These reflections showed an average linear decay of 7% over the course of data collection, for which no correction was applied. The data were processed[10] and a standard deviation was calculated for each observed intensity from the formula

$$\sigma(I) = [\mathrm{CT} + 0.25(t_c/t_b)^2(B_1 + B_2) + (pI)^2]^{1/2}$$

where CT is the integrated peak count obtained in time t_c, B_1 and B_2 are the background counts obtained in time t_b, and I is the intensity. A statistical examination of the variations in the intensities of the standard reflections suggested that a value for p, the "ignorance factor",[11] of 0.02 was appropriate. This value gave a suitable weighting scheme in later stages of refinement. Corrections for Lorentz and polarization effects were applied to the observed intensities. A total of 119 pairs of equivalent forms *h*0*l* and *h*0$\bar{l}$ were averaged, giving an agreement factor for averaging of 3.5%. An absorption correction[8] using the Gaussian method was applied to 3827 reflections with $I > 2\sigma(I)$. The maximum and minimum transmission coefficients were 0.147 and 0.120, respectively, with a linear absorption coefficient of 162.06 cm^{-1}. The equivalent forms were reaveraged, R = 3.2%. The 3416 reflections with $F^2 > 3\sigma(F^2)$ were used in the solution and refinement of the structure.

Structure Solution and Refinement

The positional parameters for the Pt atom and the two Cl atoms were determined from a three-dimensional Patterson synthesis. The remaining six nonhydrogen atoms were located by a series of structure factor and difference Fourier synthesis calculations.[8] Refinement of atomic parameters was carried out by full-matrix least-squares techniques on F minimizing the function $\sum w(|F_o| - |F_c|)^2$ where $|F_o|$ and $|F_c|$ are the observed and calculated structure factor amplitudes, respectively. The weighting factor is given by $w = 4F_o{}^2/\sigma^2(F_o{}^2)$.

The scattering factors for the Pt, N, and C atoms were those of Cromer and Waber,[12] while those for the H atom were taken from Stewart, Davidson, and Simpson.[13] The effects of anomalous dispersion of the Pt and Cl atoms were included in the calculations. The values of $\Delta f'$ and $\Delta f''$ were those of Cromer and Liberman.[14]

Preliminary refinement was carried out using the *hkl* data only. One cycle of least-squares refinement of the Pt and two Cl atoms, varying the positional and isotropic thermal parameters, resulted in values of $R_1 = \sum||F_o| - |F_c||/\sum|F_o| = 0.102$ and $R_2 = (\sum w(|F_o| - |F_c|)^2/\sum w(F_o)^2)^{1/2} = 0.111$. Two cycles of least-squares refinement of the positional and anisotropic thermal parameters for the nine nonhydrogen atoms using the absorption-corrected data reduced R_1 and R_2 to 0.038 and 0.033, respectively.

To distinguish between the two enantiomeric structures possible for the compound, the enantiomorphic structure was refined under identical conditions. Values of R_1 and R_2 obtained were 0.049 and 0.046, respectively. The R factor ratio test applied to the weighted agreement factors, R_2, shows that the second model may be rejected at the 0.005 level.[15] Further refinement was continued on the original model.

The 12 H atoms present in the molecule were evident in a difference Fourier synthesis in geometrically feasible locations. Idealized positional coordinates were computed, assuming tetrahedral coordination about both the N and C atoms, with an N–H and C–H distance of 0.95 Å. Two cycles of least-squares refinement, with the H atom contributions included, resulted in R_1 and R_2 values of 0.0357 and 0.0283. In an attempt at a refinement of the positional parameters of these atoms it was found that the geometry of the six nonmethyl H atoms was acceptable while the methyl H atoms refined to a geometry judged to be unacceptable. Also the change in the R factor produced by refining the positional parameters of the H atoms showed no significant improvement from the model with the idealized positions. Accordingly the H atoms were included in further calculations as fixed atoms in idealized positions.

An examination of F_o and F_c indicated that secondary extinction was occurring and consequently this parameter was varied in subsequent least-squares refinements. Finally, the H atom positions were recalculated for the refined model and three cycles of full-matrix least-squares refinement, with 83 variables and 3297 unique observations for which $F^2 > 3\sigma(F^2)$, converged at residuals of R_1 = 0.0352 and R_2 = 0.0277. The final value of the extinction coefficient, 2.51 (9) × 10^{-6}, corresponded to a maximum 2.8% change in F_o.

In the final cycle no parameter shift exceeded 0.01 of its estimated standard deviation. The error in an observation of unit weight is 1.92 electrons. A statistical analysis of R_2 in terms of $|F_o|$, diffractometer setting angles χ and ϕ, and $\lambda^{-1} \sin\theta$ showed no unusual trends. A difference Fourier synthesis calculated from the final structure factors contained no features of chemical significance. The highest peak, with fractional coordinates (0.252, 0.057, 0.127) had an electron

Table I. Final Atomic Positional and Thermal Parameters[a]

Atom	x	y	z	U_{11}[b]	U_{22}	U_{33}	$U_{1,2}$	$U_{1,3}$	$U_{2,3}$
Pt	0.171 30 (3)	0.127 93 (3)	0.128 96 (4)	222 (1)	218 (1)	295 (1)	−4 (1)	4 (1)	−5 (1)
Cl(1)	0.359 0 (2)	0.171 9 (2)	0.277 0 (3)	333 (11)	456 (13)	616 (13)	−34 (10)	−132 (10)	−49 (11)
Cl(2)	0.225 8 (2)	0.247 3 (2)	−0.112 5 (3)	475 (11)	393 (11)	473 (12)	−80 (9)	114 (12)	125 (12)
N(1)	0.008 5 (6)	0.078 2 (6)	0.006 0 (8)	325 (37)	324 (37)	391 (37)	−50 (31)	−14 (31)	111 (28)
N(2)	0.106 3 (6)	0.017 5 (5)	0.326 9 (8)	304 (32)	257 (30)	396 (42)	28 (27)	−33 (27)	86 (27)
C(1)	−0.077 6 (6)	0.010 0 (6)	0.127 9 (13)	261 (32)	278 (34)	411 (39)	−42 (29)	17 (43)	60 (43)
C(2)	0.009 6 (8)	−0.064 5 (7)	0.248 4 (10)	412 (45)	296 (41)	399 (44)	−23 (38)	−32 (38)	47 (34)
C(3)	−0.175 0 (10)	−0.064 6 (9)	0.027 7 (12)	483 (55)	585 (63)	675 (60)	−193 (64)	12 (57)	−5 (49)
C(4)	0.054 6 (9)	0.083 6 (10)	0.486 2 (10)	627 (64)	679 (72)	288 (44)	−14 (58)	−8 (43)	−52 (43)

[a] Estimated standard deviations in this and other tables are given in parentheses and correspond to the least significant digits. [b] $U_{ij} = \beta_{ij}/(2\pi^2 a_i^* a_j^*)A$. The values have been multiplied by 10^4. The thermal ellipsoid is given by $\exp[-(\beta_{11}h^2 + \beta_{22}k^2 + \beta_{33}l^2 + 2\beta_{12}hk + 2\beta_{13}hl + 2\beta_{23}kl)]$.

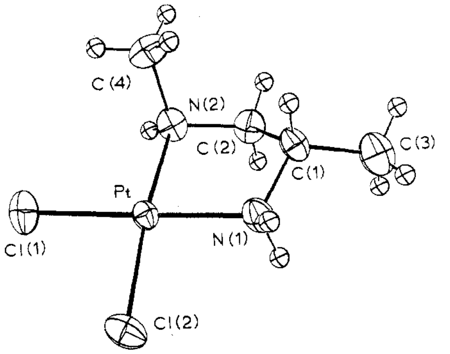

Figure 1. Perspective view of $Cl_2Pt(CH_3NHCH_2CHCH_3NH_2)$ showing the atom numbering scheme. Atoms are plotted as 50% probability ellipsoids. The H atoms have been reduced for clarity.

Table II. Derived Hydrogen Atom Positional and Isotropic Thermal Parameters

Atom	x	y	z	B,[a] Å^2
H1N(1)[b]	−0.0343	0.1489	−0.0346	472
H2N(1)	0.0289	0.0285	−0.0942	472
H1C(1)	−0.1220	0.0667	0.2009	442
H1C(2)	0.0506	−0.1258	0.1797	495
H2C(2)	−0.0387	−0.1013	0.3418	495
H1N(2)	0.1758	−0.0307	0.3671	446
H1C(3)	−0.2358	−0.0955	0.1105	712
H2C(3)	−0.2162	−0.0155	−0.0592	712
H3C(3)	−0.1330	−0.1303	−0.0307	712
H1C(4)	0.1205	0.1282	0.5433	614
H2C(4)	−0.0111	0.1378	0.4487	614
H3C(4)	0.0195	0.0268	0.5698	614

[a] The values are equivalent to 1.0 plus the isotropic B of the atom to which the H atom is bonded. The values have been multiplied by 10^2. [b] H atoms are numbered according to the atom to which they are bonded. Thus H1N(1) is bonded to N(1), etc.

Table IV. Determination of Absolute Configuration

h	k	l	$F_c(hkl)$	Obsd relationship	$F_c(hkl)$
1	10	2	19.34	<	25.29
2	6	4	29.51	<	34.06
3	2	6	19.82	<	24.52
7	4	1	18.56	<	21.76
9	6	1	20.04	<	23.11
2	2	8	17.15	>	13.02
6	6	6	16.01	<	18.46
7	3	6	16.53	<	20.65
1	1	3	61.71	<	70.91
4	5	6	22.00	<	25.17
6	2	2	34.41	>	29.41
6	4	1	37.87	>	32.39
14	3	4	18.45	<	21.20
1	4	4	18.99	≈	22.00
2	4	6	16.15	≈	13.59
3	8	2	13.99	>	17.54
3	6	6	19.27	≈	16.57
7	3	2	15.12	>	17.34

density of 0.53 (13) e Å^{-3}. Structure factors were calculated for the 400 reflections with $0 < F_o^2 < 3\sigma(F_o^2)$ which were not used in the refinement, and a statistical analysis showed no unusual trends. Only two reflections had calculated values greater than $2\sigma(F_o^2)$. Final positional and thermal parameters of the non-H atoms are given in Table I, and H atom parameters in Table II. Structure amplitudes are presented in Table III.[16]

Determination of Absolute Configuration

The choice of the absolute configuration of the molecule, determined by the Bijvoet absorption-edge technique, was confirmed by refining both models, including H atom contributions, until the refinements converged. The final model gave agreement factors of $R_1 = 0.0352$ and $R_2 = 0.0277$, while the enantiomeric structure had agreement factors of $R_1 = 0.0471$ and $R_2 = 0.0426$. The R factor ratio test when applied to R_2 shows that the second model may be rejected at the 0.005 level. Further confirmation that the correct model was chosen is given in Table IV, which lists a selection of structure amplitudes for the chosen model for which $F_c(hkl)$ and $F_c(hk\bar{l})$ differ by more than 14% based on the final positional parameters. The observed relationships confirm the correctness of the model.

Description of the Structure

A perspective view[8] of a single molecule is shown in Figure 1 which indicates the atom numbering scheme. Thermal parameters for the H atoms have been reduced to achieve clarity. Figure 2 shows the unit cell contents. There are no unusual intermolecular interactions, for the closest Pt–Pt

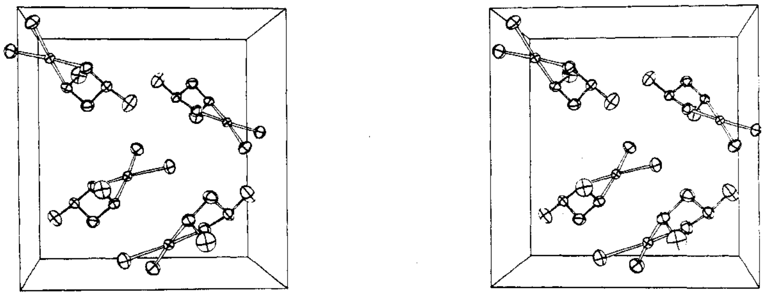

Figure 2. Stereoview of the unit cell contents. The horizontal axis, x, and the vertical axis, y, run from $-^1/_4$ to $^3/_4$. The z axis runs from 0 to 1.

Table V. Selected Intramolecular Bond Distances (Å) and Bond Angles (deg)

Distances

Pt-Cl(1)	2.306 (2)	N(2)-C(2)	1.479 (9)
Pt-Cl(2)	2.299 (2)	N(2)-C(4)	1.493 (10)
Pt-N(1)	2.013 (6)	C(1)-C(2)	1.521 (11)
Pt-N(2)	2.028 (6)	C(1)-C(3)	1.508 (12)
		C(1)-N(1)	1.484 (9)

Angles

Cl(1)-Pt-Cl(2)	92.27 (8)	Pt-N(2)-C(2)	108.2 (4)
Cl(1)-Pt-N(2)	93.84 (18)	N(1)-C(1)-C(2)	105.5 (6)
N(1)-Pt-N(2)	83.12 (24)	N(1)-C(1)-C(3)	112.8 (8)
N(1)-Pt-Cl(2)	90.75 (18)	N(2)-C(2)-C(1)	108.3 (6)
Pt-N(1)-C(1)	112.2 (5)	C(3)-C(1)-C(2)-N(2)[a]	175.6 (7)
Pt-N(2)-C(4)	113.8 (5)		

[a] A clockwise rotation of C(3) through the indicated angle superimposes it on N(2) when looking from C(1) to C(2).

Table VI. Selected Weighted Least-Squares Planes

Atoms of Plane 1 and Their Displacements from the Plane (Å)[a]

Pt	−0.0002 (3)	C(1)	−0.13
Cl(1)	0.011 (2)	C(2)	0.53
Cl(2)	0.0015 (22)	C(3)	0.39
N(1)	0.073 (7)	C(4)	−1.31
N(2)	0.013 (6)		

Atoms of Plane 2 and Their Displacements from the Plane (Å)

Pt	−0.0228	C(1)	−0.18
Cl(1)	0.005 (2)	C(2)	0.48
Cl(2)	−0.004 (2)	C(3)	0.32
N(1)	0.035 (7)	C(4)	−1.36
N(2)	−0.026 (6)		

Plane Equations of the Form $Ax + By + Cz - D = 0$

	A	B	C	D
Plane 1	4.64	−8.65	−3.24	−0.730
Plane 2	4.73	−8.58	−3.26	−0.686

[a] Displacements without esd's refer to atoms not included in the calculation of the plane.

distance of approach is 4.950 (1) Å, and the shortest intermolecular nonbonding interaction is 2.50 Å between H2N(1) and H3C(4).

The Pt–Cl distances of 2.306 (2) and 2.299 (2) Å (Table V) have a mean of 2.303 (3) Å, which agrees well with values in other structures.[17,18] When corrected for thermal motion, assuming a model in which the Cl atoms "ride" on the Pt atom, values of 2.320 (2) and 2.312 (2) Å are obtained. The mean Pt–N distance is 2.021 (8) Å. Other bond distances and angles within the chelate ring are normal.[19]

The five-membered chelate ring adopts the gauche conformation, with δ absolute configuration.[20] The methyl group on C(1) is disposed equatorially with respect to the plane of the ring, while the methyl group on N(2) adopts the axial position. The dihedral angle between the normals to the planes formed by Pt, N(1), C(1) and Pt, N(2), C(2) is 20.4 (4)°. The displacements of atoms C(1), C(2), C(3), and C(4) from the Pt, N(1), N(2) plane are 0.228 (12), −0.461 (12), −0.238 (18), and 1.320 (12) Å, respectively. Some weighted least-squares planes are given in Table VI.

Discussion

In the molecule dichloro(1-methylamino-2(*S*)-aminopropane)platinum(II) the sources of dissymmetry are restricted to a conformational contribution arising from the puckered chelate ring, vicinal contributions caused by the two asymmetric centers of the coordinated diamine, and a contribution from the distortions of the donor atoms. The optical properties of the compound are presented in Figure 3.[5] The absorption spectrum is very similar to that of *cis*-$[Pt(l\text{-}pn)Cl_2]$[21] and by analogy we can assign the absorption maxima at 33 000 and 36 500 cm^{-1} to the $^1A_1 \rightarrow {}^1A_{2g}$ and $^1A_1 \rightarrow {}^1E_g$ transitions, respectively. The absorption at 27 000 cm^{-1} has been assigned to the singlet–triplet state transitions. The circular dichroism associated with the two spin-allowed transitions has been assigned in two ways: either the two CD absorptions are due to the $^1A_2$ and E_g transitions separately or the two observed CD bands arise from the split ^1E_g components with the $^1A_{2g}$ component being superimposed on the 33 000-cm^{-1} band.[5] As has been previously observed,[2,5,22] the presence of a methyl group on a donor N atom has a dominating effect on the observed circular dichroism spectrum. The spectrum of *cis*-$[Cl_2Pt(S\text{-}pn)]$ is presented for comparison in Figure 3. If the assignment of the two circular dichroism bands at 33 000 and 37 000 cm^{-1} to the $^1A_{2g}$ and ^1E_g transitions, respectively, is adopted, then the negative ^1E_g band is strengthened, and a strong positive $^1A_{2g}$ component appears. In addition, the circular dichroism band at 27 000 cm^{-1} in *cis*-$[Cl_2Pt(S\text{-}pn)]$ is split into positive and negative components by the *N*-methyl substituent. The additivity of the ring conformational contribution, the vicinal effect of the chiral C atom, and the dominating vicinal effect of the chiral N atom have been demonstrated and used to determine conformations in related systems.[5] The absence of any strong Pt–Pt intermolecular interaction is confirmed by the similarity between the solution and solid-state circular dichroism spectra.

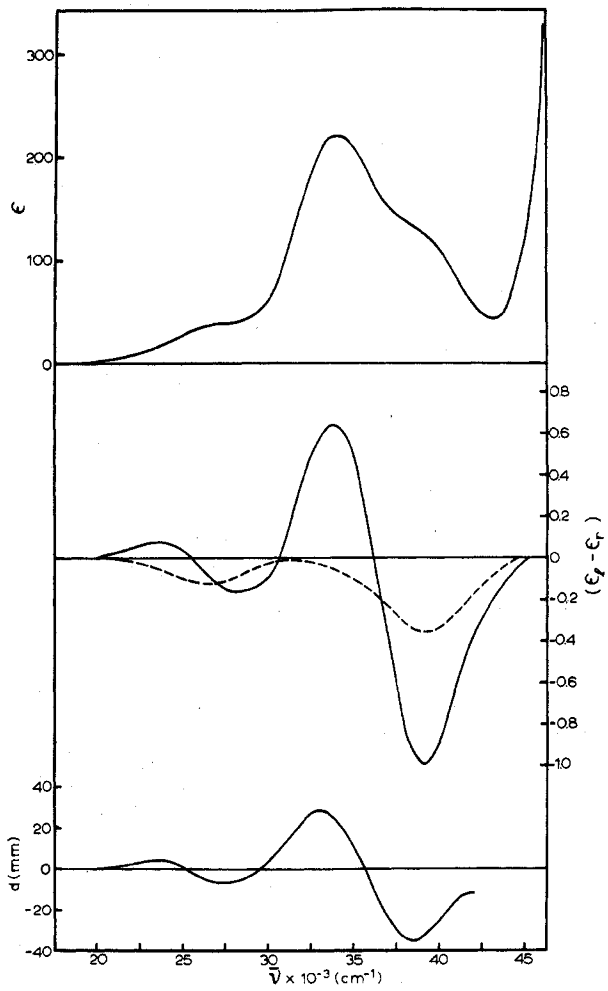

Figure 3. Absorption and CD spectra of $(-)_{280}$-$[Cl_2Pt(CH_3NHCH_2CHCH_3NH_2)]$ (——); CD solution spectrum of $[Pt(l\text{-}pn)Cl_2]$ (- - - -).

Acknowledgment. We thank the National Research Council of Canada for financial support of this work.

Registry No. (−)-*cis*-$Cl_2Pt(CH_3NHCH_2CHCH_3NH_2)$, 56323-56-9.

Supplementary Material Available: Table III, a listing of structure factor amplitudes (21 pages). Ordering information is given on any current masthead page.

References and Notes

(1) E. J. Corey and J. C. Bailar, *J. Am. Chem. Soc.*, **81**, 2620 (1959).
(2) M. Saburi, Y. Tsujito, and S. Yoshikawa, *Inorg. Chem.*, **9**, 1476 (1970).
(3) L. J. DeHayes and D. H. Busch, *Inorg. Chem.*, **12**, 1505 (1973).
(4) L. E. Erickson, M. D. Erickson, and B. L. Smith, *Inorg. Chem.*, **12**, 412 (1973).
(5) B. Bosnich and E. O. Sullivan, *Inorg. Chem.*, in press.
(6) N. C. Payne, *Inorg. Chem.*, **12**, 1151 (1973).
(7) "International Tables for X-Ray Crystallography", Vol. I, Kynoch Press, Birmingham, England, 1962.
(8) The computer programs used in this analysis include local modifications of the following: cell refinement and orientation matrix, PICKTT, from Hamilton's MODE1; full-matrix least squares, J. A. Ibers' NUCLS; Patterson and Fourier syntheses, A. Zalkin's FORDAP; function and errors, W. R. Busing, K. O. Martin, and H. A. Levy's ORFFE; crystal structure illustrations, C. K. Johnson's ORTEP; absorption correction by Gaussian integration, D. Cahen and J. A. Ibers' AGNOST. Calculations were performed on the PDP 10 and the CDC Cyber 73/14 computers at the University of Western Ontario.
(9) T. C. Furnas, "Single Crystal Orienter Manual", General Electric Co., Milwaukee, Wis., 1957.
(10) P. W. R. Corfield, R. J. Doedens, and J. A. Ibers, *Inorg. Chem.*, **6**, 197 (1967).
(11) L. E. McCandlish, G. H. Stout, and L. C. Andrews, *Acta Crystallogr.*, **31**, 245 (1975).
(12) D. T. Cromer and J. T. Waber, *Acta Crystallogr.*, **18**, 104 (1965).
(13) R. F. Stewart, E. R. Davidson, and W. T. Simpson, *J. Chem. Phys.*, **42**, 3175 (1965).
(14) D. T. Cromer and D. Liberman, *J. Chem. Phys.*, **53**, 1891 (1970).
(15) W. C. Hamilton, *Acta Crystallogr.*, **18**, 502 (1965).
(16) Supplementary material.
(17) G. H. W. Milburn and M. R. Truter, *J. Chem. Soc. A*, 1609 (1966).
(18) J. Iball, M. MacDougall, and S. Scrimgeour, *Acta Crystallogr., Sect. B*, **31**, 1672 (1975).
(19) Y. Saito, *Coord. Chem. Rev.*, **13**, 305 (1974).
(20) *Inorg. Chem.*, **9**, 1 (1970).
(21) H. Ito, J. Fujita, and K. Saito, *Bull. Chem. Soc. Jpn.*, **40**, 2584 (1967).
(22) B. Bosnich and J. M. Harrowfield, *J. Am. Chem. Soc.*, **94**, 3425 (1972).

Contribution from the Department of Chemistry,
Illinois Institute of Technology Chicago, Illinois 60616

Crystal and Molecular Structure of *uns-cis*-2,4-Pentanedionato(4,7-diaza-1,10-decanediamine)cobalt(III) Iodide Monohydrate

GEORGE R. BRUBAKER,* RAYMOND G. TELLER, and JOE N. BROWN, Jr.

Received December 9, 1975 AIC50879L

The complex *uns-cis*-2,4-pentanedionato(4,7-diaza-1,10-decanediamine)cobalt(III) iodide monohydrate, $CoC_{13}H_{31}N_4O_3I_2$, crystallizes from water in the centrosymmetric space group $P2_1/c$ with $a = 10.833$ (1) Å, $b = 12.902$ (1) Å, $c = 17.558$ (1) Å, and $\beta = 117.57$ (1)°. The calculated density of 1.85 g cm^{-3} agrees with the experimental value of 1.84 g cm^{-3} for mol wt 604 and $Z = 4$. X-ray diffraction data to $2\theta = 50°$ (Zr-filtered Mo Kα radiation) were collected with a Picker FACS-1 automated diffractometer and the structure was solved via the use of Patterson, Fourier, and least-squares refinement techniques to a final discrepancy index of 0.034 for the 3050 statistically significant ($|F_o| > 3\sigma(F_o)$) reflections. The metal ion is found at the center of a nearly regular octahedron. The structure is distinguished only by its striking similarity to that of the trans precursor and by the evidence it provides for a subtle but stereochemically significant conformation change within the ligand which must accompany trans–cis isomerization.

Introduction

As part of our continuing study of the stereochemistry of transition metal complexes with flexible tetradentate ligands, we have been impressed by the apparent stereoselectivity imparted to these species by increasing the length of the ligand chain between various pairs of donor atoms. Thus, in well-documented studies by Sargeson, Buckingham, and their co-workers,[1-3] complexes of cobalt(III) have been characterized with triethylenetetramine (3,6-diaza-1,8-octanediamine) (2,2,2-tet) in s-cis, uns-cis, and trans topologies.

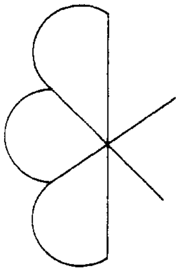

s-cis

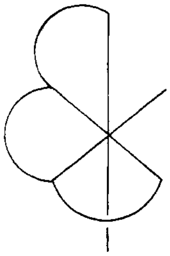

uns-cis

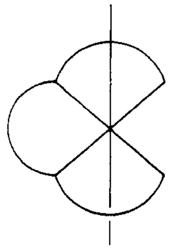

trans

Increasing the length of the chain between the secondary nitrogen donors, as in the case of 3,7-diaza-1,9-nonanediamine (2,3,2-tet) and its derivatives, favors formation of trans complexes and also leads to the exclusive formation of the uns-cis isomer.[4-6] Lengthening the chain between the primary and secondary donors [4,7-diaza-1,10-decanediamine (3,2,3-tet) and its derivatives, for example] also favors the production of trans complexes; the cis topology has only been observed for mixed-ligand complexes involving 3,2,3-tet and bidentate chelating ligands. Since the earliest reports of complexes with 3,2,3-tet, there have appeared several synthetic and spectroscopic studies supporting the uns-cis geometry for the latter complexes.[7-11] More recently, DeHayes and Busch[12] have reported the details of a strain energy minimization calculation on the *trans-* and hypothetical *cis*-Cl_2(3,2′,3-tet)Co^{III} cation from which they conclude that the trans isomers are favored by some 2.5 kcal/mol over the cis isomer and that the uns-cis complex is lower in energy than the corresponding s-cis isomer.

We report the synthesis of the *uns-cis*-2,4-pentanedionato(4,7-diaza-1,10-decanediamine)cobalt(III) cation and its electronic and ^{1}H NMR spectra in the context of the strain energy minimization calculation previously reported and of the structure of a crystal of the iodide salt.

Experimental Section

Synthesis of *uns-cis*-2,4-Pentanedionato(4,7-diaza-1,10-decanediamine)cobalt(III) Iodide Monohydrate, *uns-cis*-[Co(3,2,3-tet)acac]I_2·H_2O. To 3.4 g of *trans*-dichloro(4,7-diaza-1,10-decanediamine)cobalt(III) chloride[7] and 0.56 g of KOH dissolved in 40 ml of water at 80 °C was added 1.0 g of 2,4-pentanedione in 5 ml of